Biochimica et Biophysica Acta 1798 (2010) 1714–1723

Contents lists available at ScienceDirect

Biochimica et Biophysica Acta

journal homepage: www.elsevier.com/locate/bbamem

Interaction of 10-(octyloxy) decyl-2-(trimethylammonium) ethyl phosphate with mimetic membranes and cytotoxic effect on leukemic cells

G.A. dos Santos [a,b,1], C.H. Thomé [a,c,1], G.A. Ferreira [a,d], J.S. Yoneda [e], T.M. Nobre [f], K.R.P. Daghastanli [g], P.S. Scheucher [a,b], H.L. Gimenes-Teixeira [a,b], M.G. Constantino [e], K.T. de Oliveira [h], V.M. Faça [a], R.P. Falcão [a,b], L.J. Greene [a,c,d], E.M. Rego [a,b], P. Ciancaglini [e,*]

[a] Instituto Nacional de Ciência e Tecnologia em Células-Tronco e Terapia Celular, São Paulo, SP, Brazil
[b] Departamento de Clinica Médica, Faculdade de Medicina de Ribeirão Preto (FMRP-USP), 14051-140 Ribeirão Preto, SP, Brazil
[c] Departamento de Bioquímica, Escola Paulista de Medicina, Universidade Federal de São Paulo, 04039-002 São Paulo, SP, Brazil
[d] Departamento de Biologia Celular e Molecular e Bioagentes Patogênicos, Faculdade de Medicina de Ribeirão Preto (FMRP-USP), 14051-140 Ribeirão Preto, SP, Brazil
[e] Departamento de Química, Faculdade de Filosofia Ciências e Letras de Ribeirão Preto (FFCLRP-USP), 14040-901 Ribeirão Preto, SP, Brazil
[f] Instituto de Física de São Carlos (IFSC-USP), 13560-970 São Carlos, SP, Brazil
[g] Departamento de Bioquímica, Instituto de Química (IQ-USP), 05508-900 São Paulo, SP, Brazil
[h] Departamento de Química, Universidade Federal de São Carlos – UFSCar, Rodovia Washington Luiz, Km 235, 13565-905, São Carlos, São Paulo, Brazil

ARTICLE INFO

Article history:
Received 6 January 2010
Received in revised form 21 April 2010
Accepted 12 May 2010
Available online 19 May 2010

Keywords:
10-(Octyloxy) decyl-2-(trimethylammonium) ethyl phosphate
Lipids
Liposome
Alkylphospholipids
Leukemia

ABSTRACT

10-(Octyloxy) decyl-2-(trimethylammonium) ethyl phosphate (ODPC) is an alkylphospholipid that can interact with cell membranes because of its amphiphilic character. We describe here the interaction of ODPC with liposomes and its toxicity to leukemic cells with an ED-50 of 5.4, 5.6 and 2.9 μM for 72 h of treatment for inhibition of proliferation of NB4, U937 and K562 cell lines, respectively, and lack of toxicity to normal hematopoietic progenitor cells at concentrations up to 25 μM. The ED-50 for the non-malignant HEK-293 and primary human umbilical vein endothelial cells (HUVEC) was 63.4 and 60.7 μM, respectively. The critical micellar concentration (CMC) of ODPC was 200 μM. Dynamic light scattering indicated that dipalmitoylphosphatidylcholine (DPPC) liposome size was affected only above the CMC of ODPC. Differential calorimetric scanning (DCS) of liposomes indicated a critical transition temperature (T_c) of 41.5 °C and an enthalpy (ΔH) variation of 7.3 kcal mol^{-1}. The presence of 25 μM ODPC decreased T_c and ΔH to 39.3 °C and 4.7 kcal mol^{-1}, respectively. ODPC at 250 μM destabilized the liposomes (36.3 °C, 0.46 kcal mol^{-1}). Kinetics of 5(6)-carboxyfluorescein (CF) leakage from different liposome systems indicated that the rate and extent of CF release depended on liposome composition and ODPC concentration and that above the CMC it was instantaneous. Overall, the data indicate that ODPC acts on in vitro membrane systems and leukemia cell lines at concentrations below its CMC, suggesting that it does not act as a detergent and that this effect is dependent on membrane composition.

1. Introduction

10-(Octyloxy) decyl-2-(trimethylammonium) ethyl phosphate (ODPC) is a member of a new class of compounds, alkylphospholipids (APL), which presents anticancer and antiprotozoal activity [1]. Miltefosine and edelfosine are the most prominent representatives of this class, with miltefosine being the first drug derivative of phospholipids clinically approved for the topical treatment of skin metastases of breast cancer [2] and for the oral treatment of visceral leishmaniasis [3]. However, the efficacy of oral treatment is reduced by its gastrointestinal toxicity, which does not permit the ingestion of a dose sufficient for systemic cancer treatment. Parenteral application of miltefosine is not feasible because of hemolysis and thrombophlebitis [4].

Agresta et al. [5] compared eleven new alkylphosphocholines (APC) including ODPC to miltefosine to evaluate their hemolytic activity and cytotoxicity on non-tumoral cells (MT2). Four compounds presented lower hemolytic activity and lower cytotoxicity than miltefosine. In subsequent experiments, of these four compounds, only ODPC showed cytotoxic effects on cancer cell lines comparable to miltefosine.

The mechanism of action proposed for this class of drugs involves modulation of signaling pathways such as activation of SAPK/JNK and JNK/c-JUN and inhibition of MAPK and PI3K/Akt [4,6]. In fungi, the antiproliferative effect of edelfosine depends on selective modification of the protein composition of cell membrane lipid rafts [7]. In human leukemic cells, changes in the microenvironment of the cell membrane and capping of Fas/CD95 in membrane sub-domain rafts by edelfosine have been reported to be the mechanism that induces apoptosis [8]. Due

* Corresponding author. Tel.: +55 16 36023753; fax: +55 16 36024838.
E-mail address: pietro@ffclrp.usp.br (P. Ciancaglini).
[1] These authors contributed equally to this research.

0005-2736/$ – see front matter © 2010 Elsevier B.V. All rights reserved.
doi:10.1016/j.bbamem.2010.05.013

to their association with membranes and the modulation of diverse signaling pathways, it is possible that APL act by inducing destabilization of the plasma membrane, with the modulation of protein-function as a consequence.

In the present study, we demonstrated the cytotoxicity of 25 μM ODPC to three leukemia cell lines by inducing apoptosis within 24 h of treatment and showed that this concentration was not toxic to non-malignant cells and hematopoietic progenitor cells and determined some physicochemical properties of ODPC. An initial characterization of the interaction of ODPC with liposomes (large unilamellar vesicles, LUV) was performed. Liposome-associated cancer drugs have been reported to increase the efficacy of conventional chemotherapy by site-specific delivery [4]. We investigated the interaction of ODPC with liposomes by dynamic light scattering (DLS) measurements to determine the hydrodynamic diameter of vesicular systems. Differential scanning calorimetry (DSC) was used to determine some of the thermodynamic parameters of these systems. Finally, carboxyfluorescein (CF) leakage measurements were used to determine the effect of ODPC on membrane stability. The data reported here support the view that ODPC acts on the membrane at concentrations far below its CMC, making the membrane more fluid and unstable and this effect, as expected, is dependent on the lipid composition of the membrane. Taken together, our observations provide new information about the biological action of ODPC on models of cell membranes and about its toxic effect on malignant cells and lack of toxicity to normal cells at concentration up to 25 μM.

2. Material and methods

2.1. Materials

All solutions were prepared using Millipore DirectQ ultra pure apyrogenic water. Dipalmitoylphosphatidylcholine (DPPC), phosphate-buffered saline (PBS), Tris(hydroxymethyl)aminomethane (Tris), polidocanol, tetramethylsilane (TMS), CF, cholesterol (Chol), propidium iodide (PI) and Ficoll–Hypaque were purchased from Sigma Chemical Co. (St Louis, MO, USA). CF was converted to its sodium salt and purified [9]. Annexin-V–FITC and BrdU flow kit were purchased from BD Biosciences Pharmingen (San Diego, CA, USA). DNA was extracted using the GFX™ kit purchased from GE Healthcare (Piscataway, NJ, USA). Human recombinant cytokines (stem cell factor, FLT-3 ligand, IL-3, IL-6, GM-CSF and erythropoietin) were obtained from Stemcell Technologies (Vancouver, Canada), and egg-phospatidylglycerol (PG) was purchased from Avanti Polar Lipids, Inc. (Alabaster, AL, USA); egg-phosphatidylcholine (PC) was purified as described by Maximiano et al. [10]. All solvents and reagents used for the synthesis were purchased from commercial sources and were analytical grade or better. Pyridine was dried and distilled over CaH_2. Ethanol-free chloroform was dried over silica-gel. Tetrahydrofuran (THF) was dried over sodium/benzophenon. *N*,*N*-dimethylformamide (DMF) was dried over CaH_2, distilled from molecular sieves (3A). Phosphorus oxychloride and triethylamine were distilled before use. Silica gel 200–400 mesh (Acros, Trenton, NJ, USA) was used for preparative chromatography. Silica gel 60 F_{254} plates (Merck, Rahway, NJ, USA) were used for analytical thin layer chromatography (TLC).

2.2. Synthesis of 10-(octyloxy) decyl-2-(trimethylammonium) ethyl phosphate

ODPC, compound 5 (Scheme 1), was synthesized essentially as described by Agresta et al. [5] in the original report of its synthesis (see Supplementary material). Modifications of the synthesis were introduced in order to optimize some of the synthetic steps. All products obtained in each step were characterized by hydrogen nuclear magnetic resonance (^{1}H NMR) using a Bruker Avance 400 MHz or 500 MHz instrument. ^{1}H chemical shifts are reported in δ units (ppm) relative to TMS as internal standard and all spectra were recorded in $CDCl_3$ or $CDCl_3/CD_3OD$ (2/1). All compounds were also characterized by high resolution mass spectrometry (HRMS) ESI-TOF, in a Q-TOF Bruker instrument.

2.3. Surface tension measurements

The critical micellar concentration (CMC) of ODPC was determined by surface tension measurements using the pendant drop method based on a modified axisymmetric drop shape analysis [11], with an automatic contact-angle-tensiometer (OCA-20, Dataphysics, Bad Vilbel, Germany) as described [12]. Drops containing different concentrations of ODPC in PBS (137 mM NaCl, 2.7 mM KCl, 8.0 mM Na_2HPO_4, 1.5 mM KH_2PO_4, pH 7.4) were formed at the tip of a syringe needle in a thermostated optical glass cuvette containing water vapor-saturated air and imaged using a CCD camera. Software was used to trigger the recording of the images before the formation of the complete drop. Surface tension measurements were made on solutions of different ODPC concentrations (1.0 μM to 1.0 mM). The surface tension was then determined by digitalizing and analyzing the profile of the droplet and fitting it to the Young–Laplace equation. Surface tension was considered to be at equilibrium after reaching a constant value (<0.2 m Nm^{-1}) for at least 2 min.

2.4. Liposome preparation

LUV composed of DPPC or DPPC:Chol (molar ratio 9:1 and 9:4) were prepared as described below. Phospholipids were dissolved in chloroform and dried under nitrogen. The resulting lipid film was maintained under vacuum in a desiccator for 16 h and resuspended in PBS. The mixture was incubated for 1 h at 60 °C, above the critical phase transition temperature of the lipid, and vortexed for 10 min. LUV were prepared by submitting the suspension to extrusion (eleven times) through two 100-nm polycarbonate membranes in a LiposoFast extrusion system (Liposofast, Sigma-Aldrich). The concentration of liposomes was 1 mg/mL in each experiment in the presence or absence of the drug.

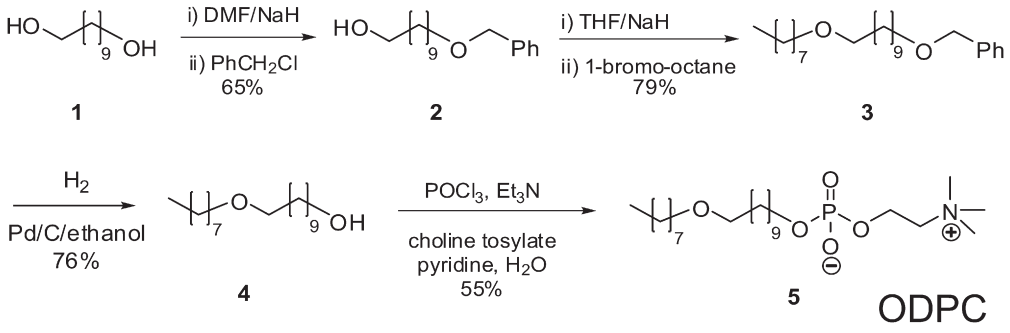

Scheme 1. Synthesis of 10-(octyloxy) decyl-2-(trimethylammonium)ethyl phosphate (ODPC), compound 5.

2.5. Dynamic light scattering measurements

The determinations of liposome size distribution were carried out by DLS, using a N5 Submicron Particle Size Analyzer (Beckman Coulter, Inc., Fullerton, CA, USA). The average value of the liposome diameters was obtained from the unimodal distribution of DPPC liposomes previously incubated at 25 °C, for 0 to 120 min, with 25 or 250 μM of ODPC.

2.6. Differential scanning calorimetry

Transition phase temperatures (T_c) of the LUV membranes prepared with different lipid compositions and in the absence or presence of ODPC were studied by DSC. LUV suspensions and the reference buffer were degassed under vacuum (140 mbar) for 15 min prior to use. The samples were scanned from 20 to 100 °C at an average rate of 1 °C/min and the recorded thermograms were analyzed using Nano-DSC II software (Calorimetry Sciences Corporation, CSC, Lindon, UT, USA).

2.7. Entrapment of carboxyfluorescein in liposomes

Liposomes containing egg-phosphatidylcholine (PC), egg-phosphatidylcholine:egg-phosphatidylglycerol (PC:PG 3:1 molar ratio) or egg-phosphatidylcholine:cholesterol (PC:Chol 3:2 molar ratio) were prepared using the extrusion system described above. CF entrapment was carried out as described by Verly at al. [13]. Briefly, a dichloromethane solution of each component of the lipid mixture was added to a tube and the solvent was evaporated under a nitrogen stream until a thin film was formed. The film was maintained under vacuum for at least 1 h to evaporate residual solvent and then rehydrated with 10 mM Tris–HCl buffer, pH 8.0, containing 50 mM CF. LUV were prepared by submitting the suspension to extrusion and free CF was removed by passing 0.25 mL of the extruded LUV through a Sephadex-G25 medium column (1.2×20 cm) eluted with 10 mM Tris–HCl buffer, pH 8.0 containing 300 mM NaCl. The LUV were collected at the Vo. The phospholipid content of the eluted LUV was determined as described by Rouser et al. [14]. Relative cholesterol concentration is reported as % cholesterol calculated on molar basis.

2.8. Dye leakage measurements due to action of ODPC on LUV membranes

Aliquots of LUV (5 μL) were added to a fluorescence cuvette containing 0.5 mL of 10 mM Tris–HCl buffer, pH 8.0, containing 300 mM NaCl. The increase of CF fluorescence as a function of time at 25 °C at several ODPC concentrations was recorded continuously in a Hitachi F-2000 Fluorescence Spectrophotometer ($\lambda_{ex}=490$ nm and $\lambda_{em}=512$ nm). At the end of each experiment, total CF fluorescence was determined after the addition of 5 μL of 10% (w/v) polidocanol which released all of the encapsulated dye. Percent CF leakage was determined as described [13].

2.9. Cell culture, cell counting and viability measurements

The human cell lines NB4 (acute promyelocytic leukemia) [15], U937 (histiocytic lymphoma with myeloid markers) [16] and K562 (chronic myeloid leukemia in blast crisis) [17] were cultured at 37 °C with 5% CO_2 in RPMI 1640 medium supplemented with 10% fetal bovine serum. The non-malignant embryonic cell line HEK-293 was cultured in DMEM medium supplemented with 20% fetal bovine serum. Primary human umbilical vein endothelial cells (HUVEC) were obtained as previously described by Covas et al. [18] with modifications, i.e., cells were cultured in EGM-2 medium (Lonza, USA) supplemented with 20% fetal bovine serum to avoid cell differentiation. All other cell lines were acquired from ATCC. Cell viability measurements of the leukemia lineages were performed with an initial minimum viability of at least 95% as determined by the Trypan blue assay [19]. Cells were counted in a Neubauer chamber in triplicate. ODPC was tested at 5, 10, 25 and 50 μM concentration for 24, 48 and 72 h, and PBS was used as the vehicle control. The concentration of 25 μM was selected for further experiments of apoptosis and cell proliferation rate because of its effect on the dose screening experiments and the lack of toxicity toward normal hematopoietic cells (see Results section). The non-malignant adherent cells in exponential growth were plated at a density of 10^5 cells per well, left to stand overnight and subsequently treated with ODPC (10, 25, 50 and 100 μM). After 24, 48 and 72 h of treatment, the culture was photographed with an Axiovert 40 inverted microscope (Zeiss, Germany), the cells were washed with PBS, trypsinized and counted in a T890 automatic cell counter (Beckman Coulter, USA). The experiments were performed in triplicate.

2.10. Apoptosis

Apoptosis was measured by three independent methods: (1) annexin-V–PI assay, (2) morphologic evaluation and (3) DNA fragmentation analysis. For the annexin-V and PI assay, 5×10^5 cells were harvested by centrifugation and resuspended in 100 μL of binding buffer (10 mM HEPES, 140 mM NaCl and 25 mM $CaCl_2$, pH 7.4) with 5 μL of annexin-V–FITC and 10 μL of 50 μg/mL PI, incubated for 20 min at room temperature and analyzed by flow cytometry (FACScalibur, Becton Dickinson Immunocytometry Systems, San Diego, CA, USA) using the Cell Quest Software (BD BioSciences, San Diego, CA, USA). For morphologic analysis, cytospin slides were prepared and Leishman stained as previously described [20].

DNA fragmentation analysis was carried out as previously described [21]. Briefly, 5×10^6 cells were treated with 25 μM ODPC or PBS for 3, 6, 12 and 24 h. Cells were harvested and DNA was extracted using the GFX™ kit following the directions of the manufacturer. Nucleic acid concentration was measured with a NanoVue nano-spectrophotometer (GE Healthcare, USA) as absorbance at 260 nm. DNA, 5 μg/sample, was submitted to electrophoresis in a 0.7% agarose gel.

2.11. Cell proliferation rate

Cell proliferation rate was measured by monitoring the incorporation of bromodeoxyuridine (BrdU) detected by flow cytometry using the BrdU flow kit (BD Pharmingen, USA) according to manufacturer instructions. Cells were treated with 25 μM ODPC or PBS as vehicle control for 24 h and exposed to 1 μM BrdU during the last 30 min of incubation, and after processing, cells were analyzed in a FacsCalibur Flow Cytometer and results analyzed with the Cell Quest Software.

2.12. Normal hematopoietic progenitor colony assay

The study was approved by the Ethics Committees of the Faculty of Medicine of Ribeirão Preto, USP, and of the Federal University of São Paulo, UNIFESP (protocol no. #1129/08), and written informed consent was obtained from all patients. Patients submitted to orthopedic surgery of the backbone due to scoliosis were the donors. All patients ($N=5$) presented normal hematologic counts and were considered to be clinically healthy except for the orthopedic disease. Bone marrow samples were collected by aspiration from the iliac crest. All samples presented a normal distribution of hematopoietic cells as evaluated by morphologic analysis (myelogram). Mononuclear cells were isolated by density gradient Ficoll–Hypaque centrifugation and counted in a Newbauer chamber. Cells were diluted in methylcellulose medium supplemented with human recombinant cytokines (stem cell factor, FLT-3 ligand, IL-3, IL-6, GM-CSF and erythropoietin) and plated onto 35-mm gridded plates. ODPC (25 or 50 μM final concentration) or PBS vehicle was added to the medium. Burst-forming units—erythroid (BFU-E), colony-forming units—erythroid (CFU-E) and colony-forming units—granulocyte and macrophage (CFU-GM) were counted after 14 days of incubation at 37° C, 5% CO_2.

3. Results

3.1. Synthesis of 10-(octyloxy) decyl-2-(trimethylammonium) ethyl phosphate

ODPC was obtained as indicated in Scheme 1. Compound 2 was synthesized by monoprotection of decanodiol (compound 1) generating the mono-alkoxide in DMF/NaH followed by the reaction with benzyl chloride and purified on a silica-gel column (65% yield relative to the previous synthetic step). Then, compound 2 was alkylated with 1-bromo-octane after alkohoxide generation (NaH/THF), giving compound 3 at 79% yield after purification on a silica-gel column. Compound 3 was deprotected with hydrogen and a C/Pd catalyst, providing compound 4 at 76% yield after purification on silica-gel column. The last step was the addition of choline performed by reacting compound 4 with $POCl_3$ and $Et_3N/CHCl_3$ and then with choline tosylate in warm pyridine (50 °C). Water was then added. Compound 5 was purified using CH_3OH:acetic acid 6:4 as eluent (55% yield) on a silica-gel column. The overall yield was 21% for compound 5. Mass spectrometry indicated a signal at 474.3319 U, which corresponds to [Molecule + Na] ion, and the signal at 490.3056 U, which corresponds to [Molecule + K] ion. Both adducts were formed during the analysis and do not indicate contamination of the ODPC. 1H-NMR analysis confirmed the homogeneity and identity of compound 5. Details of the synthesis are available in Supplementary material.

3.2. Determination of the critical micellar concentration of ODPC

The plot of surface tension *versus* ODPC concentration is given in Fig. 1. Increasing ODPC concentration decreased the surface tension. However, at approximately 200 μM ODPC, the surface tension became constant, indicating micelle formation in the bulk. Extrapolating the two lines indicates that the critical micellar concentration of ODPC was 200 μM.

3.3. Interaction of ODPC with liposomes

We studied ODPC at two concentrations to better determine the mechanism of interaction of ODPC with membranes and its possible dependence on a detergent action. The first, 25 μM, was chosen because it was effective on leukemic cells (see details below in Figs. 5–7) and not toxic to non-malignant cells or to normal hematopoietic progenitors (Fig. 8). The second 250 μM, is above the CMC of ODPC.

Dynamic light scattering (DLS) showed that DPPC-liposome size was not affected by the presence of 25 μM ODPC for up to 2 h of incubation (Fig. 2), and there were no changes in PI. However, in the presence of 250 μM ODPC, there was an increase of liposome size from 150 to 600 nm after 1 h of incubation. It is important to note that the number of liposomes with increased diameter decreased after 1 h, probably due to their rupture. The light scattering data also indicated an increase of PI for the liposome system, with a reduction in the scattering intensity, after 1 h in the presence of 250 μM ODPC. PI = 0.98 indicated heterogeneity of the liposome size range. When the same study was carried out with a liposome system prepared with different proportions of cholesterol (DPPC:cholesterol 9:1 or 9:4 molar ratio), the liposome diameters were not affected by either 25 or 250 μM ODPC.

In order to determine if the insertion of ODPC into the membrane had really occurred, a DSC assay was performed. Fig. 3 shows the DSC thermograms of liposomes of different compositions in the absence and presence of 25 and 250 μM ODPC, concentrations below and above the CMC. Only one transition temperature was observed for all systems. When ODPC was present at the concentration of 250 μM, there was a slight displacement of the T_c to lower values: 4.6, 1.3 and 0.1 °C for DPPC; DPPC:Chol (9:1) and DPPC:Chol (9:4), respectively. The data in Table 1 indicate that the variation of enthalpy (ΔH^{cal}) of ODPC and liposomes of different compositions decreased with increasing ODPC concentration, irrespective of liposome composition, showing that ODPC induced thermodynamic modifications in the lipid bilayers. This phenomenon is also demonstrated in Fig. 3, where increased concentrations of ODPC reduced the heat capacity of the liposomes in a concentration-dependent manner.

The composition of the liposomes had an even greater effect on ΔH^{cal} when one considers only the concentration of 25 μM (far below the CMC of 200 μM). In liposomes composed of DPPC:cholesterol (9:4), a composition closer to that present in biological systems, the effect on ΔH^{cal} was more pronounced. In addition to DPPC (Fig. 3A) and DPPC:Chol (9:1) (Fig. 3B), the width at half height of peak ($\Delta T_{1/2}$) was greater when ODPC was present at a concentration above the CMC (200 μM) (Table 1). However, this increase was not observed with DPPC:Chol (9:4) (Fig. 3C), a relative concentration of cholesterol that led to a significant broadening of the peaks, thus forming systems less stable than the others.

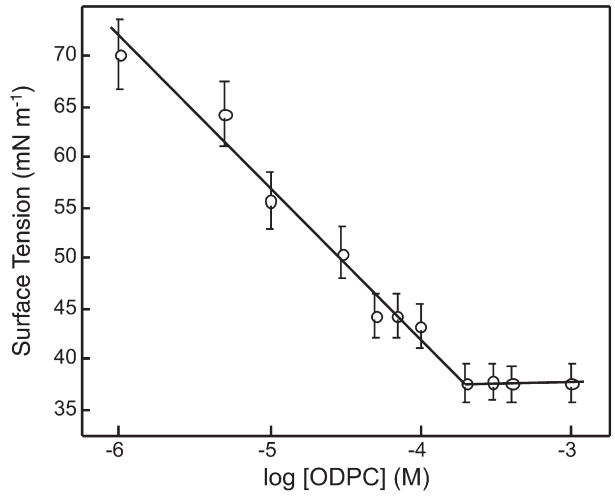

Fig. 1. Effect of ODPC concentration on surface tension. The surface tension measurements were carried out in 5 mM Tris–HCl buffer, pH 7.0, containing 150 mM KCl at 25 °C. Data are reported as means ± SD for 5 measurements per point. The critical micellar concentration was 200 μM ODPC.

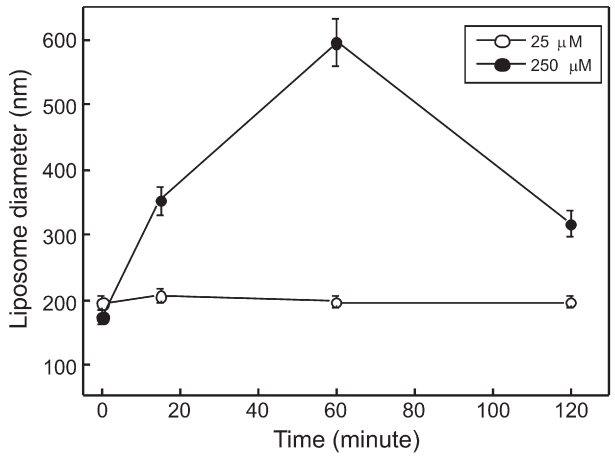

Fig. 2. Effect of ODPC on liposome diameters. Data are reported as means ± SD for 3 measurements. Average values of the liposome diameters were obtained by dynamic light scattering (unimodal distribution) of DPPC liposomes incubated at 25 °C for different periods of time with (○) 25 and (●) 250 μM ODPC.

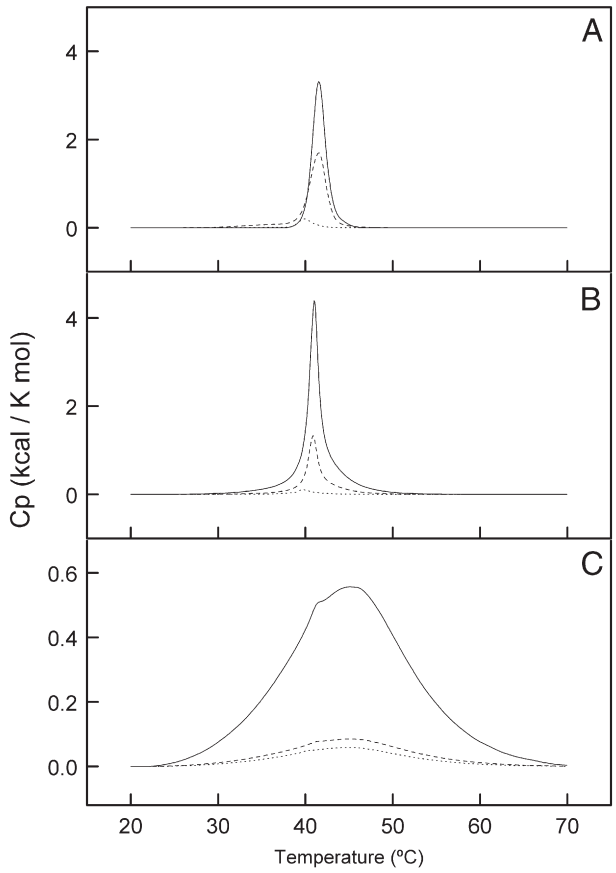

Fig. 3. Differential scanning calorimetry (DSC) thermograms of liposomes in the absence and in the presence of ODPC. DSC thermograms were determined using an N-DSC II calorimeter and the result is reported as Cp (kcal/K.mol) as a function of temperature (°C). The liposomes were (A) DPPC, (B) DPPC:Cholesterol 9:1 molar ratio and (C) DPPC:Cholesterol 9:4 molar ratio, in the absence (—) and in the presence of 25 (- - -) and 250 μM (·····) ODPC.

3.4. Membrane permeabilization

The rate of CF leakage from the vesicles was measured by the increase of fluorescence emission as a function of time in order to study the membrane permeabilization after ODPC insertion. CF is self-quenched at high concentrations such as that trapped inside the liposomes used in these experiments. Fig. 4 shows the kinetics of CF leakage from PC, PC:PG (3:1) and PC:Chol (3:2) LUV. CF leakage of less than 4% ODPC was observed for all liposome systems studied when up to 50 μM ODPC was used or when ODPC was absent (see Table 2).

All kinetic curves were obtained after the addition of 100 μM ODPC (below the CMC). This ODPC concentration promoted a 59% leakage of CF from PC LUV within 18 min. Other ODPC concentrations were tested (200, 400 and 600 μM) and showed similar leakage rates for the same period independently of the ODPC concentration (Table 2). It is important to note that even when using an ODPC concentration at or above the CMC (3-fold CMC), the leakage was not complete during the 20 min studied.

Table 1
Effect of ODPC concentration and lipid composition on thermodynamic values describing the interaction with liposomes.

Liposomes	ODPC (μM)	T_c (°C)	ΔH^{cal} (kcal mol^{-1})	ΔH decrease (%)[a]	$\Delta T_{1/2}$ (°C)
DPPC	0	41.5	6.80	—	1.60
	25	41.5	4.44	34.7	1.70
	250	36.9	0.483	92.9	1.95
DPPC:Chol (9:1)	0	41.0	11.5	—	1.65
	25	40.9	3.03	73.7	1.64
	250	39.7	0.329	97.1	2.69
DPPC:Chol (9:4)	0	45.0	9.95	—	13.8
	25	45.1	1.50	85.0	13.8
	250	44.9	1.01	89.8	13.4

[a] Decrease of ΔH with respect to the control (absence of ODPC).

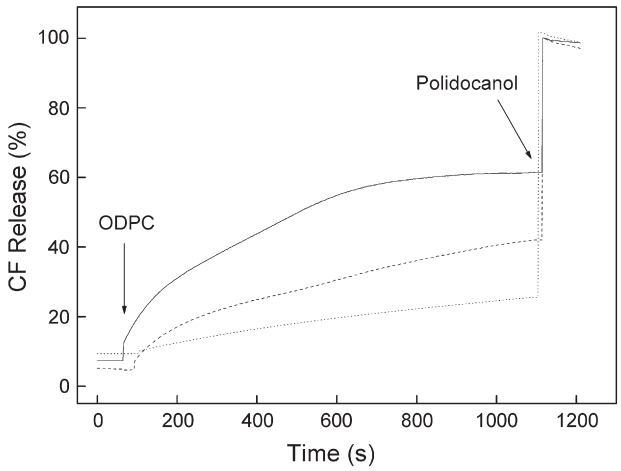

Fig. 4. Effect of ODPC on carboxyfluorescein leakage from liposomes of different compositions. The concentration of added ODPC (arrow) was 100 μM and the liposome composition was PC (—); PC:PG 3:1 molar ratio (- - -); PC:Chol 3:2 molar ratio (·····). Arrows indicate the time of addition of ODPC and polidocanol, respectively.

The effect of the negative charge of the liposome membrane on the permeabilization activity of ODPC was studied using LUV consisting of PC:PG (3:1 mol ratio) and monitoring the increase of CF fluorescence during its leakage (Fig. 4). For 100 μM ODPC, the CF leakage was 39% within 18 min. The permeabilization caused by the addition of 400 μM ODPC was about 48% as summarized in Table 2. These results suggest a decrease of membrane permeability in the presence of a negative charge. Also, an expressive decrease (17%) in CF leakage to 100 μM ODPC was observed for PC:Chol (3:2) (a concentration below CMC) compared to the other LUV preparations (Table 2).

3.5. Cytotoxic screening assays (cell counting and viability) on leukemic cells

In order to determine the concentration at which ODPC was effective, we measured cell proliferation and viability using three representative cell lines of acute myeloid leukemia, i.e., NB4, U937 and K562. In a screening experiment, treatment with 25 μM ODPC for 24 h induced a decrease of approximately 50–60% in the proliferation of NB4 and U937 cell lines (Fig. 5). The K562 cell line was more resistant in the first 24 h (Fig. 5). However, after 48 and 72 h of treatment, the three cell lines showed similar sensitivity and a low viability rate in response to 25 μM ODPC even at lower ODPC concentrations (Fig. 5). Table 3 presents the estimated ED-50 for each cell line at 24, 48 and 72 h.

Table 2
CF Leakage from LUV composed of PC, PC:PG (3:1 molar ratio) and PC:Chol (3:2 molar ratio) in the absence or presence of ODPC.

ODPC (μM)	CF leakage (%)		
	PC	PC:PG	PC:Chol
0	0.03	0.02	0.02
25	2.06	1.11	1.92
50	3.52	1.12	3.22
100	58.8	39.2	17.0
200	62.9	50.1	23.3
400	61.5	48.9	18.9
600	64.1	44.6	17.7

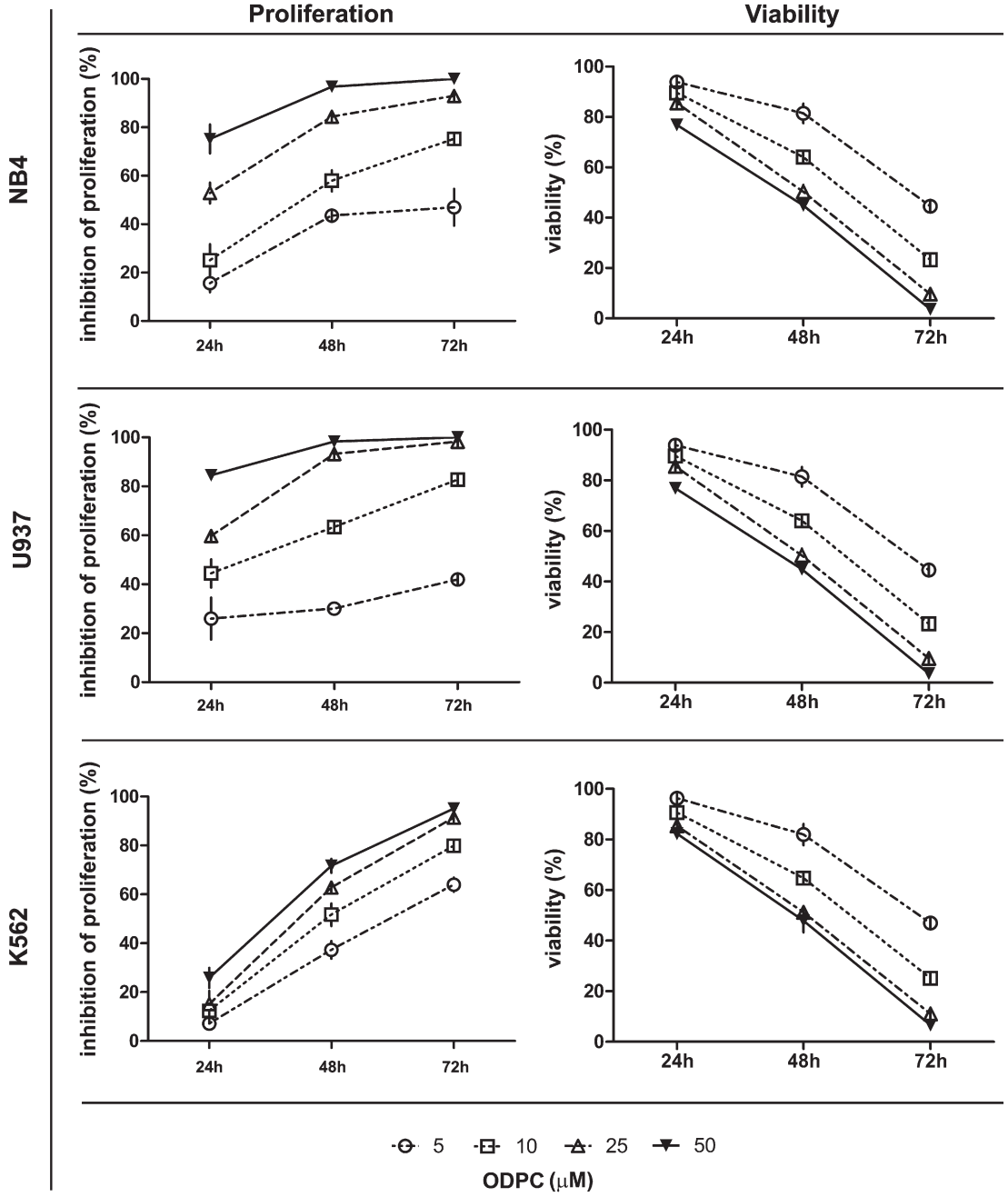

Fig. 5. ODPC reduces the proliferation and viability of cultured leukemia cells. Cells in exponential growth were plated at a concentration of 5×10^5 cells/ml and treated with ODPC or PBS vehicle. In the upper panels, NB4 (acute promyelocytic leukemia); central panels, U937 (histiocytic lymphoma with myeloid markers); lower panels, K562 (chronic myeloid leukemia in blast crisis). The concentrations of ODPC are indicated by the symbols and time is given on the abscissa. In the left row, cell proliferation was determined by cell counting in a Neubauer chamber. The results are reported as percent inhibition of proliferation compared to control. In the right row, viability was evaluated by Trypan blue exclusion dye assay. The experiments were carried out in triplicate and data are reported as mean ± SD. When error bars are not given, they are smaller than the symbols.

Table 3
Effective dose (ED) 50% of ODPC for the inhibition of the proliferation of leukemic and non-malignant cells.

	24 h			48 h			72 h		
	ED-50 (μM)	95% CI	R^2	ED-50 (μM)	95% CI	R^2	ED-50 (μM)	95% CI	R^2
NB4	22.12	19.35 to 25.30	0.9617	6.737	5.930 to 7.653	0.9663	5.357	4.857 to 5.909	0.9726
U937	13.89	11.81 to 16.34	0.9466	7.581	7.372 to 7.796	0.9977	5.629	5.509 to 5.751	0.9976
K562	186.4	132.3 to 262.4	0.9596	10.43	8.813 to 12.34	0.9419	2.937	2.548 to 3.386	0.9809
HEK-293	99.49	90.56 to 109.3	0.9575	75.58	72.09 to 79.24	0.9898	63.44	58.65 to 68.61	0.9787
HUVEC	98.06	87.77 to 109.6	0.9474	73.75	68.47 to 79.43	0.9762	60.68	55.11 to 66.82	0.9689

95% CI is the 95% confidence interval for ED-50, expressed as μM.
R^2 is the goodness of fit coefficient.

3.6. Anti-proliferative action of ODPC and induction of apoptosis in leukemic cells

After 24 h, 25 μM ODPC induced apoptosis and inhibited the proliferation rate of NB4 and U937 cell lines. The incorporation of BrdU (Fig. 6), a marker of DNA synthesis and S phase of the cell cycle, confirmed a high sensitivity of the leukemic cell lines to ODPC as demonstrated in Fig. 4. The assays of apoptosis (phosphatidylserine externalization and DNA fragmentation analysis) revealed the same tendency. An extensive DNA fragmentation pattern was detected as

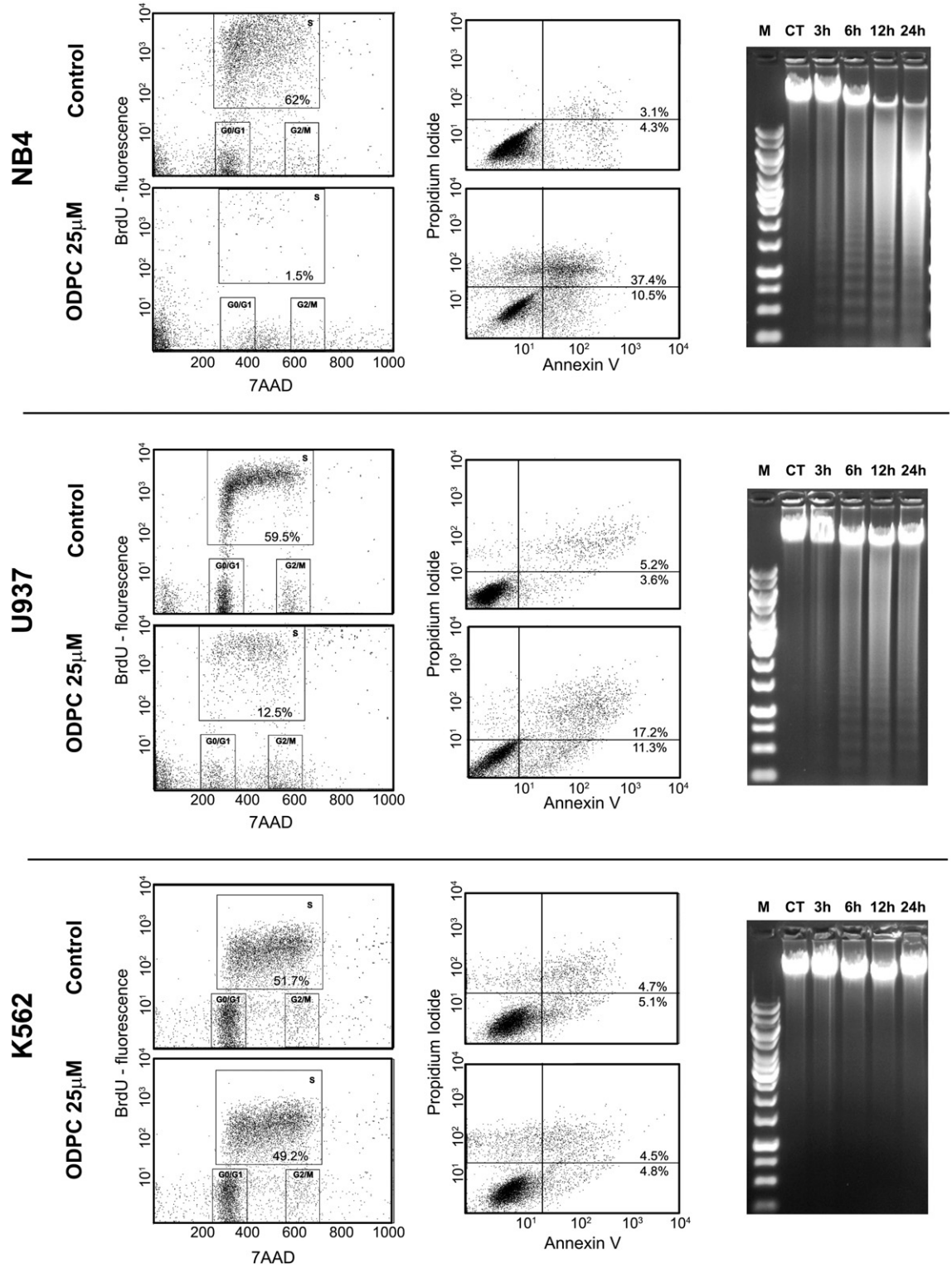

Fig. 6. Proliferation rate and apoptosis of cultured leukemia cells treated with ODPC. Cells in exponential growth were plated at a concentration of 5×10^5 cells/ml and treated with ODPC or PBS vehicle for 24 h or the indicated periods of time. Upper panel, NB4; middle panel, U937; lower panel, K562. The cells were treated with 25 μM ODPC for the times indicated in the figure. Proliferation rate was evaluated by BrdU incorporation (left row), and cell cycle analysis was carried out with the DNA-specific dye 7-AAD. The gates show the cell cycle phases G1, S and G2/M. In the middle panel, apoptosis was evaluated by phosphatidylserine externalization, with cells positive for annexin-V considered to be apoptotic. Numbers indicate the percent of cells in each gate. DNA fragmentation electrophoretic analysis is shown in the right row. Data are representative of three independent experiments.

early as 6 h after treatment with 25 μM ODPC in the more sensitive cell lines NB4 and U937 compared to K562 (Fig. 6). We confirmed the pro-apoptotic action of ODPC also by morphologic analysis that showed pycnotic nuclei and membrane blebbing in a significant fraction of cells (Fig. 7).

3.7. Effect of ODPC on non-malignant cells

ODPC at concentrations up to 25 μM was not toxic to the growth of HEK-293 (embryonic kidney cells, Fig. 8A) and to a primary HUVEC (Fig. 8B); however, the concentrations of 50 and 100 μM showed toxicity to both cells. Microscopic evaluation confirmed the results (Supplemental Figs. 1 and 2). Estimated ED-50 for both cells at 24, 48 and 72 h treatment are presented in Table 3.

3.8. Effect of ODPC on normal hematopoietic progenitors

We performed a methylcellulose-based hematopoietic progenitor colony assay to evaluate the toxicity of ODPC to normal hematopoietic cells. ODPC (25 μM) did not change the proliferation or differentiation of normal hematopoietic progenitors as shown in Fig. 8C. However, the concentration of 50 μM was toxic to these cells and induced a reduction of approximately 50% in the number of colonies in relation to control (Fig. 8C).

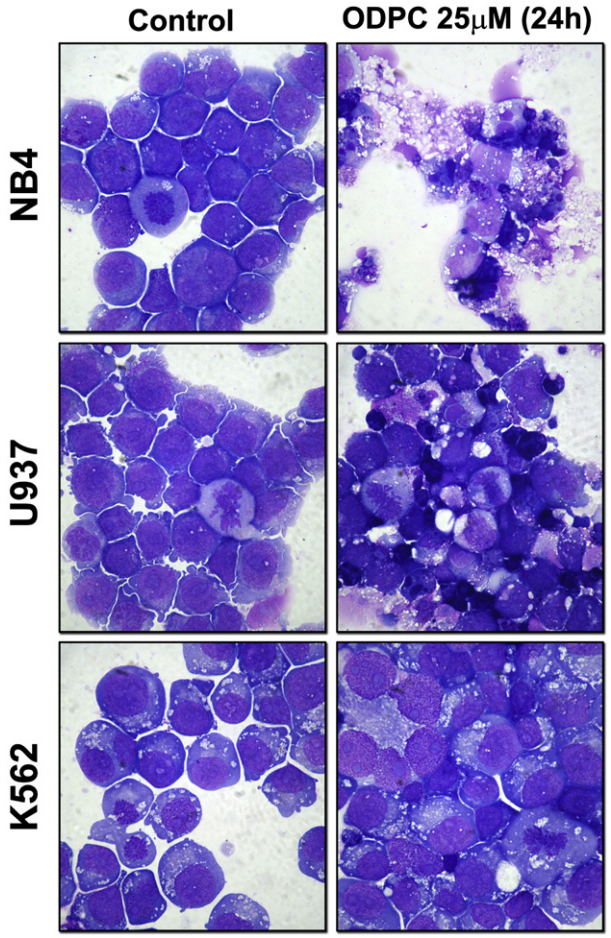

Fig. 7. Morphologic analysis of the effect of 25 μM ODPC on cultured leukemia cells. Cells in exponential growth were plated at a concentration of 5×10^5 cells/ml and treated with ODPC or PBS vehicle for 24 h. In the upper panels, NB4 (acute promyelocytic leukemia); central panels, U937 (histiocytic lymphoma with myeloid markers); lower panels, K562 (chronic myeloid leukemia in blast crisis). The vehicle control is in the left row and cells treated with 25 μM ODPC are in the right row. The characteristic membrane blebbing and the nuclear condensation, morphologic hall markers of apoptosis, are seen especially in the NB4 and K562 samples treated with ODPC. Representative experiment of three independent experiments.

4. Discussion

It has been proposed that the APL family of drugs interacts with cell membranes due to their amphiphilic character; however, the exact mechanism and the possible dependence on a detergent action have not been clarified. Their probable alignment at interfaces reflects the tendency of ODPC to assume the most energetically favored orientation and to act as a detergent. Detergent-based cell lysis (and consequent death) is a general phenomenon that would not be expected to be specific and toxic only to cancer cells. Indeed, this non-specific mechanism may be responsible for the gastrointestinal toxicity of miltefosine at high doses [3].

In order to determine if the toxicity of ODPC against cancer cells was dependent on a detergent action, we first evaluated its CMC. ODPC presented a CMC of 200 μM determined by surface tension measurements. The compound closest to ODPC in structure found in the literature is octadecyl trimethyl ammonium chloride (OTAC), which also contains 18 carbons in the alkyl chain. This cationic amphiphilic compound has a CMC of 190 μM [12], which is close to that of ODPC, 200 μM. Comparing OTAC and ODPC, their equivalent CMCs indicate that the polar head groups can present similar size and the extension of the alkyl chain is determinant for micelle formation.

The results of biological assays demonstrated that 25 μM ODPC was toxic to leukemic cells but not to normal hematopoietic cells. At this point it is important to notice that methylcellulose-based hematopoietic colony assay is a validated procedure that is capable of predicting the maximum tolerated dose *in vivo* [22–24]. The demonstration of apoptosis excludes a cytostatic effect in the treatments with 25 μM ODPC. Apoptosis is a common consequence of exposure of cancer cells to effective chemotherapeutic agents [25,26]. In addition, the results with the embryonic kidney cell line HEK-293 and with HUVEC demonstrate that ODPC, at concentrations that are toxic to leukemia cells, spares non-malignant cells of a non-hematopoietic origin.

Our results can be compared with those obtained by Agresta et al. [5] who estimated the ED50 for 48 h treatment of ODPC at more than 100 and 68 μM for inhibition of proliferation of K562 cells using the MTT and ^{3}H thymidine assays, respectively. In the present study, we have estimated the same ED50 at 10.43 μM but we have used another method, i.e., microscopic cell counting. Differences in the methods used or in the basal state of growth of the cell line may explain this discrepancy.

To characterize ODPC, we evaluated its interaction with liposomes that are used as models for the study of biological membranes. Liposomes have many physicochemical properties similar to those of cell membranes such as membrane permeability, osmotic activity and interaction with various solutes, surface characteristics and chemical composition [27]. The fluidity of their membranes and their self-closing structure are essential parameters for the study of biological membrane function. The DSC measurements of thermodynamic parameters of the interaction with liposomes are important to identify changes of structural and physicochemical characteristics of lipid bilayers caused by drugs [27]. With this model system, we were able to obtain several indications of how ODPC disturbs liposome structure.

Our results indicated that the incorporation of ODPC into DPPC and DPPC:Chol bilayers (Fig. 3) caused a reduction in the variation of ΔH^{cal} and T_c, indicating that ODPC destabilized the liposome (Table 1). The decrease of ΔH^{cal} was greater when ODPC was incorporated into the lipid bilayer at a concentration above the CMC, indicating that this modification was concentration dependent. Moreover, 25 μM ODPC, a concentration demonstrated to be cytotoxic to leukemic cells and far below the CMC, induced a significant reduction of ΔH^{cal} in relation to PBS vehicle control. Furthermore, this effect was dependent on the lipid composition of liposomes and was greater when cholesterol was present in the preparation (Table 1). This result is consistent with the

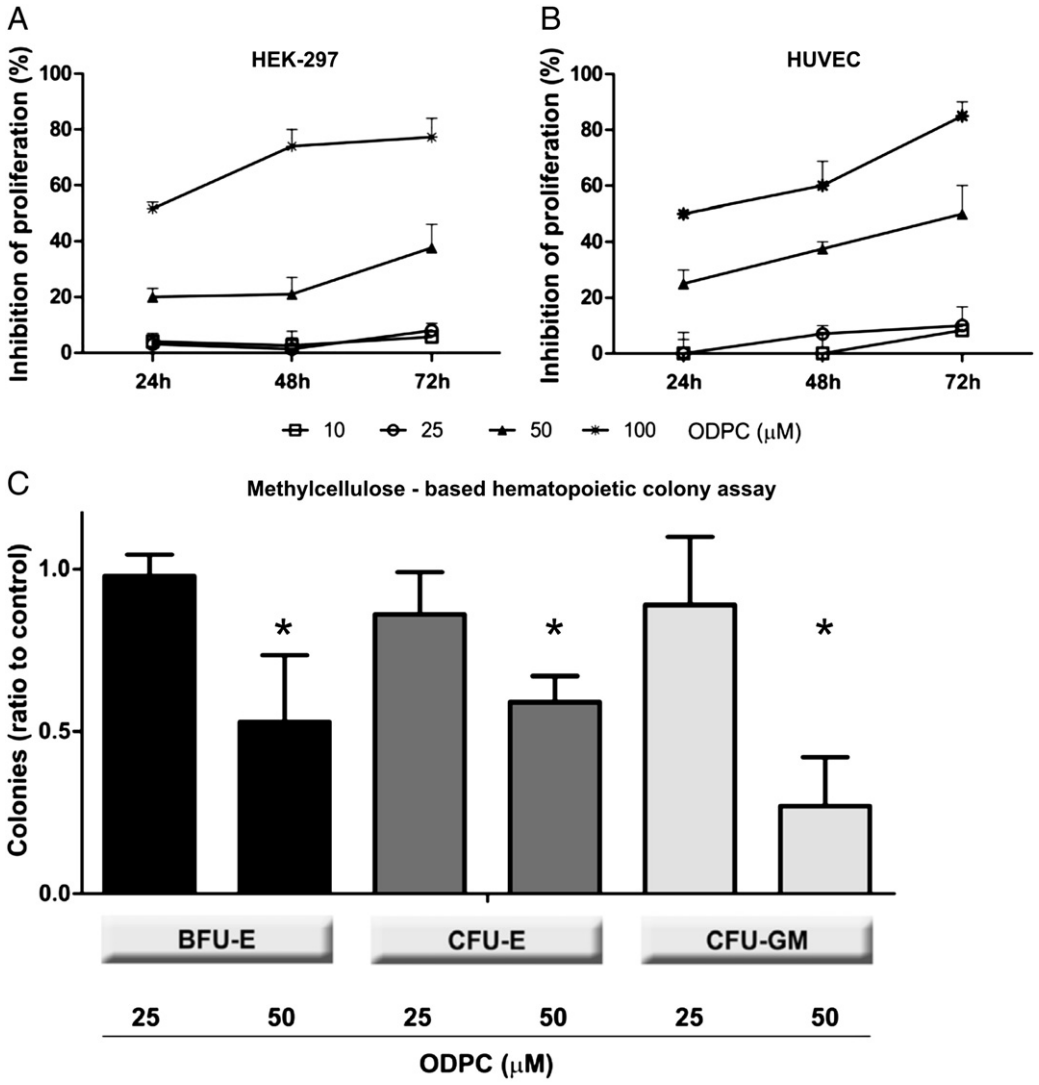

Fig. 8. Evaluation of ODPC toxicity to non-malignant cells and to normal hematopoiesis. (A) Embryonic kidney cells (HEK-293) and (B) primary human umbilical vascular endothelial cells (HUVEC) were cultured and treated as described in Section 2.9. The concentrations of ODPC are indicated by the symbols and time is given on the abscissa. Results are reported as a normalized inhibition of proliferation in relation to the PBS-treated control. (C) The procedure of methylcellulose-based hematopoietic colony assay from normal donor bone marrow samples is described in Section 2.12. Colonies were counted after 14 days. Number of colonies was normalized to control (PBS vehicle) as an ODPC/control ratio, with values significantly lower than 1 indicating toxicity. BFU-E: burst-forming units—erythroid; CFU-E: colony-forming units—erythroid; CFU-GM: colony-forming units—granulocyte and macrophage. *$P<0.05$ compared to control (one-way ANOVA followed by Dunnett's multiple comparison test between control and 25 or 50 μM treated samples for each type of cell).

hypothesis that APL may preferentially interact with highly organized sub-domains named rafts [28] that are rich in cholesterol [29]. Indeed it has been proposed that normal raft assembly may be essential to signaling transduction in the plasma membrane [30].

The strong effect on the enthalpy in the transition indicates that the ODPC must be inside the hydrophobic interior of the phospholipid array and not superficially in the vicinity of the polar groups or at the interface of the phospholipids [31]. Furthermore, Table 1 shows that the $\Delta T_{1/2}$ for 250 μM ODPC is greater than that for 25 μM ODPC and that this increase is more significant for DPPC:Chol at a molar ratio of 9:1, indicating that the presence of cholesterol leads to greater destabilization, decreasing the cooperativity of the system. Fig. 3C shows that cholesterol at a molar ratio of 9:4 led to a significant broadening of the peaks and the incorporation of ODPC did not change $\Delta T_{1/2}$ values. Therefore, cholesterol was responsible for the destabilization of phospholipid assemblies.

To further study the properties of ODPC related to the hemolytic activity of APC, we performed studies of permeabilization in membrane systems composed of PC, PC:PG or PC:Chol. Only at ODPC concentrations below the CMC did the leakage present a kinetic behavior with a progressive increase in CF leakage (Fig. 4). Using ODPC concentrations above 200 μM, an instantaneous leakage occurred, which was constant during the experiment (data not shown). This effect was probably due to the fact that the ODPC molecule inserted into the membrane caused a transitory perturbation and fast leakage. The membrane then returns to equilibrium and the leakage becomes slower or stops. Furthermore, in negative membranes, the total CF leakage during the same period was smaller than that observed for PC LUV. This effect could be due to (i) columbic interactions among the polar phospholipid head groups that reduced membrane leakage or (ii) the high hydration in the interface region caused by the negative charges present in the phosphate group.

In addition to the negative charge effect, the permeabilization action of ODPC was also studied in the presence of a membrane prepared with a PC:Chol 3:2 molar ratio (Table 2), a condition proposed to be the closest to the erythrocyte membrane, with 41 mol% cholesterol [13,32]. In this case, any increase of ODPC concentration (Table 2 and Fig. 4) added to membrane samples had less effect on membrane permeabilization compared to PC and even PC:PG LUV. Actually, it is well known that the presence of cholesterol can change the lipid packing and increase its rigidity. This result is consistent with the report of Agresta et al. [5] who described

ODPC as an APL with minor hemolytic activity, a result that may represent a significant advantage in future clinical trials.

In the present study, we demonstrated that ODPC induced cell death primarily by apoptosis and inhibited proliferation in three human leukemia cell lines in the concentration range of 10 to 50 μM that is far below the CMC. Interestingly, Agresta et al. [5] determined the IC-50 of ODPC against MT2 cells (a non-tumoral cell line) to be greater than 100 μM, and the hemolytic activity for the same compound was demonstrated only with concentrations above 2 mM.

The physicochemical data obtained in the present study indicate that the interaction of ODPC with mimetic PC membranes occurs even below the CMC. DLS, DSC and CF leakage revealed that the insertion of ODPC into the membrane destabilized it, making it more fluid. The use of liposomes as a model for cell membranes showed that ODPC may interact with membranes at low concentrations without causing rupture.

Acknowledgements

The authors thank Prof. Dr. Stefano Servi, Dipartimento di Chimica, Materiali, Ingegneria Chimica "Giulio Natta," Politecnico di Milano and CNR, Istituto di Chimica del Riconoscimento Molecolare "Adolfo Quilico," Italy, for providing a sample of the original compound that was used as a standard for comparison with ODPC synthesized in our laboratory and Maristela D. Orellana and Alexandre Krause for technical assistance with HUVEC cells and HEK-293 cells, respectively. The authors also thank the following Brazilian governmental agencies for financial support: Conselho Nacional de Desenvolvimento Científico e Tecnológico (CNPq), Coordenação de Aperfeiçoamento do Pessoal de Ensino Superior (CAPES), Fundação de Amparo a Pesquisa do Estado de São Paulo (2008/06619-4) and Fundação de Apoio ao Ensino, Pesquisa e Assistência do Hospital das Clínicas da FMRP-USP (FAEPA). Thanks are also due to Prof. Norberto Pepoline Lopes for High Resolution Mass Spectroscopy (ESI) analyses.

Appendix A. Supplementary data

Supplementary data associated with this article can be found, in the online version, at doi:10.1016/j.bbamem.2010.05.013.

References

[1] S.L. Croft, K. Seifert, M. Duchêne, Antiprotozoal activities of phospholipid analogues, Mol. Biochem. Parasitol. 126 (2003) 165–172.
[2] S. Clive, J. Gardiner, R.C.F. Leonard, Miltefosine as a topical treatment for cutaneous metastases in breast carcinoma, Cancer Chemother. Pharmacol. 44 (1999) S29–S30.
[3] S.K. Bhattacharya, T.K. Jha, S. Sundar, C.P. Thakur, J. Engel, H. Sindermann, K. Junge, J. Karbwang, A.D.M. Bryceson, J.D. Berman, Efficacy and tolerability of miltefosine for childhood visceral leishmaniasis in India, Clin. Infect. Dis. 38 (2004) 217–221.
[4] L.H. Lindner, M. Hossann, M. Vogeser, N. Teichert, K. Wachholz, H. Eibl, W. Hiddemann, R.D. Issels, Dual role of hexadecylphosphocholine (miltefosine) in thermosensitive liposomes: active ingredient and mediator of drug release, J. Control. Release 125 (2008) 112–120.
[5] M. Agresta, P. D'Arrigo, E. Fasoli, D. Losi, G. Pedrocchi-Fantoni, S. Riva, S. Servi, D. Tessaro, Synthesis and antiproliferative activity of alkylphosphocholines, Chem. Phys. Lipids 126 (2003) 201–210.
[6] C. Gajate, A. Santos-Beneit, M. Modolell, F. Mollinedo, Involvement of c-Jun NH2-terminal kinase activation and c-Jun in the induction of apoptosis by the ether phospholipid 1-*O*-octadecyl-2-*O*-methyl-rac-glycero-3-phosphocholine, Mol. Pharmacol. 53 (1998) 602–612.
[7] V. Zaremberg, C. Gajate, L.M. Cacharro, F. Mollinedo, C.R. McMaster, Cytotoxicity of an anti-cancer lysophospholipid through selective modification of lipid raft composition, J. Biol. Chem. 280 (2005) 38047–38058.
[8] C. Gajate, F. Mollinedo, The antitumor ether lipid ET-18-OCH3 induces apoptosis through translocation and capping of Fas/CD95 into membrane rafts in human leukemic cells, Blood 98 (2001) 3860–3863.
[9] J. Weinstein, S. Yoshikami, P. Henkart, R. Blumenthal, W. Hagins, Liposome-cell interaction: transfer and intracellular release of a trapped fluorescent marker, Science 195 (1977) 489–492.
[10] F.A. Maximiano, M.A. da Silva, K.R.P. Daghastanli, P.S. de Araujo, H. Chaimovich, I. M. Cuccovia, A convenient method for lecithin purification from fresh eggs, Quim. Nova 31 (2008) 910–913.
[11] P. Cheng, D. Li, L. Boruvka, Y. Rotenberg, A.W. Neumann, Automation of axisymmetric drop shape analysis for measurements of interfacial tensions and contact angles, Colloids Surf. 43 (1990) 151–167.
[12] H.-U.K. Kye-Hong Kang, K.-H. Lim, N.-H. Jeong, Mixed micellization of anionic ammonium dodecyl sulfate and cationic octadecyl trimethyl ammonium chloride, Bull. Korean Chem. Soc. (BKSC) 22 (2001) 1009–1014.
[13] R.M. Verly, M.A. Rodrigues, K.R.P. Daghastanli, A.M.L. Denadai, I.M. Cuccovia, C. Bloch, F. Frezard, M.M. Santoro, D. Pilo-Veloso, M.P. Bemquerer, Effect of cholesterol on the interaction of the amphibian antimicrobial peptide DD K with liposomes, Peptides 29 (2008) 15–24.
[14] G. Rouser, S. Fleischer, A. Yamamoto, Two dimensional thin layer chromatographic separation of polar lipids and determination of phospholipids by phosphorus analysis of spots, Lipids 5 (1970) 494–496.
[15] M. Lanotte, V. Martinthouvenin, S. Najman, P. Balerini, F. Valensi, R. Berger, NB4, a maturation inducible cell-line with T(15-17) marker isolated from a humam acute promyelocitic leukemia (ME), Blood 77 (1991) 1080–1086.
[16] F.N. Strefford, J.C., T. Chaplin, M.J. Neat, R.T. Oliver, B.D. Young, L.K. Jones, The characterisation of the lymphoma cell line U937, using comparative genomic hybridisation and multi-plex FISH, , 2001, pp. 9–14.
[17] S. Naumann, D. Reutzel, M. Speicher, H.J. Decker, Complete karyotype characterization of the K562 cell line by combined application of G-banding, multiplex-fluorescence in situ hybridization, fluorescence in situ hybridization, and comparative genomic hybridization, Leuk. Res. 25 (2001) 313–322.
[18] D.T. Covas, J.L.C. Siufi, A.R.L. Silva, M.D. Orellana, Isolation and culture of umbilical vein mesenchymal stem cells, Braz. J. Med. Biol. Res. 36 (2003) 1179–1183.
[19] S.A. Altman, L. Randers, G. Rao, Comparison of trypan blue-dye exclusion and fluorometric assays for mammalian-cell viability determinations, Biotechnol. Prog. 9 (1993) 671–674.
[20] R.A. Freitas, G.A.S. dos Santos, H.L.G. Teixeira, P.S. Scheucher, A.R. Lucena-Araujo, A.S.G. Lima, R. Lima, A.B. Garcia, A.A. Jordao, R.P. Faicao, H. Vannucchi, E.M. Rego, Apoptosis induction by (+)alpha-tocopheryl succinate in the absence or presence of all-trans retinoic acid and arsenic trioxide in NB4, NB4-R2 and primary APL cells, Leuk. Res. 33 (2009) 958–963.
[21] B. Bellosillo, M. Dalmau, D. Colomer, J. Gil, Involvement of CED-3/ICE proteases in the apoptosis of B-chronic lymphocytic leukemia cells, Blood 89 (1997) 3378–3384.
[22] A. Pessina, B. Albella, M. Bayo, J. Bueren, P. Brantom, S. Casati, C. Croera, G. Gagliardi, P. Foti, R. Parchment, D. Parent-Massin, G. Schoeters, Y. Sibiril, R. Van Den Heuvel, L. Gribaldo, Application of the CFU-GM assay to predict acute drug-induced neutropenia: an international blind trial to validate a prediction model for the maximum tolerated dose (MTD) of myelosuppressive xenobiotics, Toxicol. Sci. 75 (2003) 355–367.
[23] R.E. Parchment, M. Gordon, C.K. Grieshaber, C. Sessa, D. Volpe, M. Ghielmini, Predicting hematological toxicity (myelosuppression) of cytotoxic drug therapy from in vitro tests, Ann. Oncol. 9 (1998) 357–364.
[24] D. Moneta, C. Geroni, O. Valota, P. Grossi, M.J.A.d. Jonge, M. Brughera, E. Colajori, M. Ghielmini, C. Sessa, Predicting the maximum-tolerated dose of PNEU-159548 (4-dimethoxy-3â ²-deamino-3â ²-aziridinyl-4â ²-methylsulphonyl-daunorubicin) in humans using CFU-GM clonogenic assays and prospective validation, Eur. J. Cancer (Oxford, England: 1990) 39 (2003) 675–683.
[25] M. MacFarlane, Cell death pathways—potential therapeutic targets, Xenobiotica 39 (2009) 616–624.
[26] J. Hu, J. Fang, Y. Dong, S.J. Chen, Z. Chen, Arsenic in cancer therapy, Anticancer Drugs 16 (2005) 119–127.
[27] C. Demetzos, Differential scanning calorimetry (DSC): a tool to study the thermal behavior of lipid bilayers and liposomal stability, J. Liposome Res. 18 (2008) 159–173.
[28] C. Gajate, F. Mollinedo, Edelfosine and perifosine induce selective apoptosis in multiple myeloma by recruitment of death receptors and downstream signaling molecules into lipid rafts, Blood 109 (2007) 711–719.
[29] L.J. Pike, Rafts defined: a report on the keystone symposium on lipid rafts and cell function, J. Lipid Res. 47 (2006) 1597–1598.
[30] M.F. Hanzal-Bayer, J.F. Hancock, Lipid rafts and membrane traffic, FEBS Lett. 581 (2007) 2098–2104.
[31] L.Y. Zhao, S.S. Feng, N. Kocherginsky, I. Kostetski, DSC and EPR investigations on effects of cholesterol component on molecular interactions between paclitaxel and phospholipid within lipid bilayer membrane, Int. J. Pharm. 338 (2007) 258–266.
[32] M.K. Jain, R.C. Wagner, Introduction to biological membranes, John Wiley & Sons, USA, 1980.